Annals of Botany **111**: 467–477, 2013
doi:10.1093/aob/mcs268, available online at www.aob.oxfordjournals.org

ANNALS OF BOTANY
Founded 1887

On the complementary relationship between marginal nitrogen and water-use efficiencies among *Pinus taeda* leaves grown under ambient and CO_2-enriched environments

Sari Palmroth[1,2,*], Gabriel G. Katul[1,3], Chris A. Maier[4], Eric Ward[1], Stefano Manzoni[1,3] and Giulia Vico[3,5]

[1]*Nicholas School of the Environment, Box 90328, Duke University, Durham, NC 27708, USA,* [2]*Department of Forest Ecology and Management, Swedish University of Agricultural Sciences, SE-901 83 Umeå, Sweden,* [3]*Civil and Environmental Engineering Department, Box 90287, Duke University, Durham, NC 27708-0287, USA,* [4]*Southern Research Station, USDA Forest Service, 3041 Cornwallis Road, Research Triangle Park, NC 27709, USA and* [5]*Department of Crop Production Ecology, Swedish University of Agricultural Sciences, SE-750 07 Uppsala, Sweden*
** For correspondence. E-mail sari.palmroth@duke.edu*

Received: 29 August 2012 Revision requested: 11 October 2012 Accepted: 14 November 2012 Published electronically: 8 January 2013

• *Background and Aims* Water and nitrogen (N) are two limiting resources for biomass production of terrestrial vegetation. Water losses in transpiration (E) can be decreased by reducing leaf stomatal conductance (g_s) at the expense of lowering CO_2 uptake (A), resulting in increased water-use efficiency. However, with more N available, higher allocation of N to photosynthetic proteins improves A so that N-use efficiency is reduced when g_s declines. Hence, a trade-off is expected between these two resource-use efficiencies. In this study it is hypothesized that when foliar concentration (N) varies on time scales much longer than g_s, an explicit complementary relationship between the marginal water- and N-use efficiency emerges. Furthermore, a shift in this relationship is anticipated with increasing atmospheric CO_2 concentration (c_a).
• *Methods* Optimization theory is employed to quantify interactions between resource-use efficiencies under elevated c_a and soil N amendments. The analyses are based on marginal water- and N-use efficiencies, $\lambda = (\partial A/\partial g_s)/(\partial E/\partial g_s)$ and $\eta = \partial A/\partial N$, respectively. The relationship between the two efficiencies and related variation in intercellular CO_2 concentration (c_i) were examined using A/c_i curves and foliar N measured on *Pinus taeda* needles collected at various canopy locations at the Duke Forest Free Air CO_2 Enrichment experiment (North Carolina, USA).
• *Key Results* Optimality theory allowed the definition of a novel, explicit relationship between two intrinsic leaf-scale properties where η is complementary to the square-root of λ. The data support the model predictions that elevated c_a increased η and λ, and at given c_a and needle age-class, the two quantities varied among needles in an approximately complementary manner.
• *Conclusions* The derived analytical expressions can be employed in scaling-up carbon, water and N fluxes from leaf to ecosystem, but also to derive transpiration estimates from those of η, and assist in predicting how increasing c_a influences ecosystem water use.

Key words: Elevated CO_2, FACE, fertilization, leaf gas exchange, nitrogen, optimal stomatal conductance, pine, *Pinus taeda*, water-use efficiency.

INTRODUCTION

Ecosystem productivity and carbon storage in plant biomass are essential components of global carbon balance but their estimates remain highly uncertain. Both processes are controlled by soil nitrogen (N) availability, which determines the rate of production of different biomass compartments (McMurtrie and Wolf, 1983). In turn, foliar N concentration (N) influences leaf photosynthetic capacity (Field and Mooney, 1986; Evans, 1989). Because soil N availability is often limited and acquiring it has a cost (Bloom *et al.*, 1992), N and carbon are invested in upper canopy foliage where the return (in terms of CO_2 uptake) is larger because light is not limiting photosynthesis (e.g. Field, 1983; Anten *et al.*, 1995; Kull and Kruijt, 1999; Dewar *et al.*, 2012; Peltoniemi *et al.*, 2012). This pattern explains most of the variability of within-canopy N per unit leaf area (N_a) at a given atmospheric CO_2 concentration (c_a).

Actual leaf CO_2 uptake depends not only on leaf biochemistry (demand for CO_2) but also on the diffusion rate of CO_2 from the atmosphere through stomata to the carboxylation sites (CO_2 supply). The diffusion rate reflects the concentration gradient driving CO_2 uptake and the degree of stomatal opening, which impacts stomatal conductance (g_s). The CO_2 gradient is generally enhanced by elevated c_a and increased N allocation to photosynthetic enzymes (that reduce the concentrations of CO_2 at carboxylation sites and hence in the leaf air space, c_i). However, elevated c_a decreases stomatal opening in some species (Medlyn *et al.*, 2001), and reduction of g_s limits CO_2 uptake and reduces transpirational water loss at the scale of the leaf. In addition, under elevated c_a, the relationship between photosynthetic capacity of leaves and N may shift due to acclimation of photosynthetic biochemistry, resulting in smaller N investment in carboxylation-related proteins (reviewed by Ainsworth and

Rogers, 2007). Also, where N availability is high, more of it can be invested in the photosynthetic machinery even where light is somewhat limiting (i.e. lower in the canopy). Together, such changes may alter the distribution of N down the canopy and, thus, N- and water-use efficiencies and their interaction.

Leaf water-use efficiency (WUE $= A/E$, where A is leaf CO_2 exchange rate and E is transpiration rate) and photosynthetic N-use efficiency (PNUE $= A/N$) have been shown to inversely correlate among plant species growing along a water availability gradient (Field, 1983); species from the driest sites had the highest WUE but the lowest PNUE, because decreasing stomatal conductance in drier conditions improves WUE (for a given leaf N), but reduces PNUE by lowering the CO_2 supply to the photosynthetic sites. Accordingly, a trade-off between these two resource-use efficiencies is expected. A number of subsequent field studies showed similar patterns across a range of water and/or N availabilities among and within species (e.g. DeLucia and Schlesinger, 1991; Cernusak *et al.*, 2008; Han, 2011). To explain plant water- and N-use strategies, Wright *et al.* (2003) hypothesized that plants may adopt an 'optimal input mix' for water and N; in other words, they allocate their resource acquisition and use to minimize the total cost at a given carbon gain. The theoretical predictions combined with observations suggested that, when compared with plants in humid environments, plants in dry habitats, where N may be 'cheaper' than water, tend to operate at higher N and photosynthetic rate at a given g_s. This increase in N results in a decrease in PNUE (i.e. the relative increase in A is smaller than that in N) and the difference in WUE depends on the actual g_s and atmospheric demand for water. By extension, in a given climate, the species/individuals with easier access to N may operate at higher foliar N but similar stomatal conductance and, hence, at lower photosynthetic N-use efficiency and higher water-use efficiency.

The links among photosynthesis, transpiration and foliar N content can be described based on the economics of leaf gas exchange, where resource-use efficiencies are defined in marginal terms that are intrinsic to the leaf and vary less with climatic conditions than the flux-based WUE and PNUE. Marginal water-use efficiency is thus formally defined as $\lambda = (\partial A/\partial g_C)/(\partial E/\partial g_C)$, where g_C is stomatal conductance for CO_2 (the difference in the diffusivities of CO_2 and water vapour is accounted for in the calculation of E), and marginal N-use efficiency as $\eta = \partial A/\partial N$. Relying on the concept of a constant marginal water-use efficiency, the stomatal optimality hypothesis states that plants adjust their stomatal opening to maximize their carbon gain at a given water loss (Cowan and Farquhar, 1977; Hari *et al.*, 1986) and N status (Buckley *et al.*, 2002). Stomatal responses to variability in environmental factors (e.g. water-vapour deficit or atmospheric CO_2) are results of the optimal solution of the objective function and need not be defined *a priori*. Although co-optimization schemes of N and water use to maximize carbon gain have been proposed (Farquhar *et al.*, 2002; McMurtrie *et al.*, 2008; Dewar *et al.*, 2009), an explicit link between leaf-scale marginal N and water-use efficiencies is still lacking. Such a link would provide a framework for assessing how stomatal control relates to leaf properties within and across species and along environmental gradients.

Carbon and water exchange of leaves in response to varying CO_2 and N supply and methods of up-scaling are used in ecosystem carbon–water–nitrogen models, including large-scale climate models to assess the effects of elevated atmospheric CO_2 and N deposition on regional carbon fluxes and atmospheric CO_2 concentrations (Bonan, 2008). The incorporation of leaf-level functions to large-scale models has been made possible through remotely sensed estimates of canopy N, mapped over regions and continents (Ollinger *et al.*, 2008), and within-canopy radiative transfer and resource (C and N) allocation schemes. Stomatal conductance of leaves, based on the optimality hypothesis, offers an alternative for the current semi-empirical formulations in ecosystem models (Launiainen *et al.*, 2011; Manzoni *et al.*, 2011*a*). Moreover, such an up-scaling scheme can also be employed to study how variations in intrinsic variables of leaves, such as marginal water and N-use efficiencies, are reflected in 'effective' canopy (or big-leaf) properties and gas exchange by ecosystems. These 'canopy-level' functions are likely to be more easily incorporated in or used to constrain large-scale models.

In this work, we hypothesize that when the timescale of variation of g_C is much shorter than those of N variations for leaves operating at optimal g_C, there will be an explicit relationship between the marginal water and N-use efficiency. This expression differs from previous trade-off hypotheses between N and water use because (*a*) it is based on a complementary relationship among intrinsic variables (η and λ), and (*b*) this relationship is a consequence of optimal stomatal regulation on short time scales and the difference in timescale between N and water use. It has been shown previously that, at a given stomatal conductance and N, when photosynthesis is primarily limited by the amount and activity of Rubisco, increasing c_a increases λ (Katul *et al.*, 2010; Manzoni *et al.* 2011*b*). Increasing c_a increases c_i and shifts their relationship so that λ and η both increase. To test this complementarity hypothesis, and to study how the relationship may be affected by soil N additions, we quantified the variability of N, and water-use efficiencies among leaves using gas-exchange measurements (A–c_i curves) collected at different times and canopy positions in the *Pinus taeda* stand of the Duke Forest Free Air CO_2 Enrichment (FACE) experiment. At Duke FACE trees were grown under a split-plot design of elevated atmospheric CO_2 (+ 200 μmol mol^{-1}) and soil N amendments.

Our analysis focuses on time scales commensurate with the averaging times typical of gas-exchange measurements (i.e. hours). This is different from assessing how these resources are used by an individual plant over longer time scales (e.g. biomass growth), which requires longer integration times and accounting for changes in biomass and its partitioning (Dewar *et al.*, 2009). We use the optimality model and data simultaneously as a diagnostic tool to interpret the measured leaf gas exchange, assuming leaves are operating within the confines of optimality theory. Previous gas-exchange studies on *P. taeda* and *P. sylvestris* trees suggest that leaves tend to operate near their optimal stomatal conductance irrespective of climatic conditions and c_a (Palmroth *et al.*, 1999; Katul *et al.*, 2010). Here, we further assume that the measured gas-exchange rates reflect growth conditions of the needles, and assess the effects of elevated c_a and N availabilities on the derived relationship between η and λ.

MATERIALS AND METHODS

Theory

CO_2 uptake–stomatal conductance relationship. Mass transfer of CO_2 and water vapour through leaves occurs via Fickian diffusion effectively described as

$$A = g_C(c_a - c_i) \quad (1)$$

$$E = g_W(e_i - e_a) \approx g_W D \quad (2)$$

where c_a and c_i are the ambient and intercellular CO_2 concentrations, respectively, g_C is the stomatal conductance to CO_2, g_W is conductance to water vapour, e_i and e_a are the intercellular and ambient water-vapour concentrations, respectively, and D is the vapour-pressure deficit approximating $e_i - e_a$. Because of the difference in relative diffusivity of water vapour and CO_2, $g_W = 1\,6 g_C$. Boundary-layer conductance is assumed to be much larger than stomatal conductance, which is typical in the cuvette-based gas-exchange measurements used in this study. Hence, leaf temperature can be well approximated by air temperature.

Equation (1) describes the rate of CO_2 supplied from the atmosphere to the leaf at a given c_i, where c_i depends on the balance between this atmospheric CO_2 supply and demand by the photosynthetic biochemistry. The CO_2 demand can be generically expressed as (Farquhar *et al.*, 1980)

$$A = \frac{a_1(c_i - \Gamma^*)}{c_i + a_2} - R_d \quad (3)$$

where Γ^* is the CO_2 compensation point in the absence of mitochondrial respiration, a_1 and a_2 are kinetic constants that depend on whether photosynthesis is limited by ribulose-1,5 biphosphate (RuBP) regeneration rate or Rubisco activity, and R_d is the daytime mitochondrial respiration rate. Under light-saturated conditions, as in all gas-exchange measurements used in this study, $a_1 = V_{c,max}$ (maximum carboxylation rate of Rubisco) and the half-saturation constant is $a_2 = K_C(1 + C_O/K_O)$ (where K_C and K_O are the Michaelis–Menten constants for CO_2 fixation and oxygen inhibition, respectively, and C_O is the oxygen concentration in air). These expressions for a_1 and a_2 are valid when mesophyll conductance (g_m) is non-limiting. Should g_m become important, the value of a_1 can be interpreted as a 'macroscopic' kinetic constant that also accounts for any leaf internal diffusive limitations.

Whenever $\Gamma^* \ll c_i$, the demand function (eqn 3) may be simplified by noting that c_i in the denominator can be broken down into a long-term mean value, i.e. $c_i = rc_a$, where r is a constant and its fluctuations assumed to be much smaller than a_2. This assumption is reasonable for light-saturated conditions given that $a_2 > c_i$. Expressed in terms of g_C and upon neglecting R_d relative to A (as is the case for large A), eqn (1) and the linearized demand function can be combined to yield an A–g_C relationship independent of c_i (see Lloyd, 1991; Katul *et al.*, 2010)

$$A = \frac{g_c a_1 c_a}{a_1 + g_c(a_2 + rc_a)} \quad (4)$$

It is noted that eqn (4) retains the non-linear relationship between A and c_a despite the linearized A–c_i.

Marginal water-use efficiency. The theoretical optimal g_C is derived from the maximization of the objective function $f(g_C) = A(g_C) - \lambda E(g_C)$, where $\lambda = (\partial A/\partial g_C)/(\partial E/\partial g_C)$ is the marginal water-use efficiency (Hari *et al.*, 1986; Lloyd, 1991). By inserting eqns (2) and (4) into $f(g_C)$, a λ_{LI} (where LI refers to the linearized demand function) can be computed for $\partial f(g_C)/\partial g_C = 0$ as

$$\lambda_{LI} = \frac{c_a}{aD}\left(1 - \frac{c_i}{c_a}\right)^2 \quad (5)$$

Moreover, the flux-based WUE may be expressed as a function of λ_{LI} as

$$\mathrm{WUE} = \frac{A}{E} = \sqrt{\frac{\lambda_{LI} c_a}{aD}} \quad (6)$$

A number of studies have shown that λ_{LI} increases almost linearly with c_a [i.e. $\lambda_{LI} = \lambda_o\,(c_a/c_o)$, where λ_o reflects the marginal water-use efficiency of the leaf grown at c_o] and results in a quasi-linear increase of WUE with c_a at a given D (Buckley, 2008; Katul *et al.*, 2009, 2010; Barton *et al.*, 2012; Manzoni *et al.*, 2011*b*). Note, however, that the sensitivity of λ_{LI} to c_a in the solution of the optimal conductance depends on the assumed limiting condition of photosynthesis in the objective function. In line with the gas-exchange measurements carried out in this study, our formulation of optimal g_C (Katul *et al.*, 2010) uses the Rubisco-limited function of the biochemical model (Farquhar *et al.*, 1980) and results in λ_{LI} increasing with c_a. This differs from the formulation by Medlyn *et al.* (2011), where photosynthesis is assumed to be limited by RuBP regeneration, so that λ_{LI} (or their 'water cost of carbon', corresponding to $1/\lambda_{LI}$ using our notation) is insensitive to c_a. Despite the apparent contrast in the predictions of changes in marginal water-use efficiency with atmospheric c_a between these two approximations of optimal stomatal conductance, both recover the linear relationship between g_C and A/c_a used in semi-empirical models (Launiainen *et al.*, 2011; Volpe *et al.*, 2011; Way *et al.*, 2011) and both suggest that stomatal conductance of *P. taeda* is insensitive to c_a.

Marginal N-use efficiency. The derivation of λ can be modified to include the simultaneous costs of using water (at a given rate of E) and N (Buckley *et al.*, 2002). Due to the difference in time scale between variations in g_C (fast) and N (slow), λ variations for a given foliar N content can be assessed without concerns about their joint interactions in the cost function. The marginal N-use efficiency η (see Farquhar *et al.*, 2002) can be defined as

$$\eta = \partial A/\partial N \quad (7)$$

Because the majority of N is invested in photosynthesis-related proteins, photosynthetic capacity and $V_{c,max}$ are often tightly correlated with total N (Evans, 1989). The slope of the A–N relationship reflects N investment among various photosynthesis-

related and structural pools in the leaf (Field and Mooney, 1986). It may vary seasonally and with growth conditions such as c_a or light availability (Niinemets and Tenhunen, 1997; Crous and Ellsworth, 2004).

When the range in the observed values of N is wide enough, the $A-N$ and $V_{c,max}-N$ relationships tend to saturate (Evans, 1989). Based on fertilization experiments, this saturation has been attributed to decreasing Rubisco activation state, or $V_{c,max}$/Rubisco ratio (Cheng and Fuchigami, 2000; Warren *et al.*, 2003). Thus, in a given light environment, increasing N availability may not affect the fractional allocation to Rubisco, but more N may be accumulated as photosynthetically inactive 'storage-Rubisco'. In the following, the 'photosynthetically active' N is thus denoted by N_p, and the total N expressed on the total needle surface area basis, N_a. The most elementary representation of this type of saturation effect is to assume N_p increases proportionally to N_a, up to a transition N_a, above which N_p remains constant.

Using eqn (3), the formulation for eqn (7) can be expanded in terms of photosynthetic parameters to yield

$$\begin{aligned}\eta &= \frac{\partial A}{\partial N_a} = \frac{\partial A}{\partial a_1}\frac{\partial a_1}{\partial N_p}\frac{\partial N_p}{\partial N_a} + \frac{\partial A}{\partial c_i}\frac{\partial c_i}{\partial N_p}\frac{\partial N_p}{\partial N_a} \\ &= \frac{\partial N_p}{\partial N_a}\left[\frac{\partial A}{\partial a_1}\frac{\partial a_1}{\partial N_p} + \frac{\partial A}{\partial c_i}\frac{\partial c_i}{\partial N_p}\right] \\ &= \frac{\partial N_p}{\partial N_a}\frac{1}{c_i + a_2}\left[(c_i - \Gamma^*)\frac{\partial a_1}{\partial N_p} + a_1\frac{a_2 + \Gamma^*}{c_i + a_2}\frac{\partial c_i}{\partial N_p}\right] \\ &\qquad\qquad T_1 \qquad\qquad T_2\end{aligned} \tag{8}$$

where T_1 accounts for variations in c_i with g_C and A, as well as the change in a_1 with respect to N_p, and T_2 accounts for possible variations in c_i originating solely from N_p. When a change in N_p causes a smaller relative change in c_i than in a_1 (here $V_{c,max}$) the ratio of T_2 to T_1, expressed as $(\delta c_i/c_i)/(\delta a_1/a_1)$, becomes much smaller than unity. When stomata regulate their aperture to maximize A at given E, the c_i at the optimum g_C does not vary with a_1 (or N) as shown in eqn (5) so that $\partial c_i/\partial N_p = 0$. As a result, eqn (8) reduces to a simpler form that includes T_1 only. Hence, when $(\delta c_i/c_i)/(\delta a_1/a_1)$ approaches unity, stomata may not be operating 'optimally' in the carbon-gain and water-loss economy, and the joint optimization problem with N included becomes necessary.

In addition to N availability affecting the activation state of Rubisco (through $\partial N_p/\partial N_a$), the activation state may also change with leaf age in response to a decrease in CO_2 supply to chloroplasts (Ethier *et al.*, 2006), yet is not affected by c_a (Rogers and Ellsworth, 2002). Elevated c_a may, however, induce changes in $\partial a_1/\partial N_p$ through Rubisco-specific down-regulation. The values of a_1, a_2 and Γ^* (eqn 3) as well as $\partial a_1/\partial N_p$ also vary with leaf temperature (T_L). We described the dependence of a_1 (= $V_{c,max}$ under saturating light) on T_L based on common formulations such as those in Campbell and Norman (1998), and we modelled $V_{c,max}$ at 25 °C as

$$V_{c,max25}(25\,^\circ\mathrm{C}, N_p) \approx s_1 N_p + s_2 \tag{9}$$

where s_1 and s_2 are parameters that describe the sensitivity of $V_{c,max25}$ to N_p. The differentiation of eqn (9) with respect to N_p yields $\partial V_{c,max}/\partial N_p \approx s_1(T_L)$, where only the effect of the slope s_1 is retained.

Linking marginal N-use efficiency with marginal water-use efficiency. Combining the simplified photosynthesis model with the version of eqn (8) accounting for T_1 only (i.e. optimal stomatal regulation) results in

$$\eta_{LI} = \frac{c_i}{a_2 + rc_a}\frac{\partial a_1}{\partial N_p}\frac{\partial N_p}{\partial N_a} = \frac{c_i/c_a}{a_2/c_a + r}\frac{\partial a_1}{\partial N_p}\frac{\partial N_p}{\partial N_a} \tag{10}$$

where c_i/c_a varies as $1 - \sqrt{(\lambda_{LI} a D/c_a)}$ (eqn 5) and, therefore, λ_{LI} and η_{LI} can be related through

$$\eta_{LI} = \frac{1 - \sqrt{\lambda_{LI} a D/c_a}}{a_2/c_a + r}\frac{\partial a_1}{\partial N_p}\frac{\partial N_p}{\partial N_a} \tag{11}$$

This expression shows that, when stomata are operating optimally $[\partial f(g_C)/\partial g_C = 0]$, for a given temperature-dependent $\partial V_{c,max}/\partial N_p$ and at a given D and c_a, η_{LI} and $\lambda_{LI}^{1/2}$ are complementary, as η_{LI} increases and λ_{LI} decreases with increasing c_i (eqn 5). Increasing c_a will increase both λ_{LI} and η_{LI}. These relationships are explored using the experiments described next.

Experimental data

Setting. The Duke FACE experiment is located within a *Pinus taeda* plantation (established in 1983) in the Blackwood Division of Duke University's Duke Forest, in Orange County, North Carolina, USA (35°58′N, 79°08'W). Summers are warm and humid and winters are moderate. The mean annual temperature and precipitation are 15 5 °C and 1145 mm, respectively. The soil is moderately low-fertility, acidic clayey-loam of the Enon series.

This study is based on data collected from the FACE prototype, FACEp (the first elevated CO_2 plot and its reference plot) and the replicated FACE experiment (three additional plot pairs) In FACEp, CO_2 enrichment started in 1994 (targeted up to 550 μmol mol^{-1}), and in 1996 in the three additional elevated FACE plots (targeted at +200 μmol mol^{-1}). In 1998, FACEp plots were split in half by an impermeable barrier and one-half of each was fertilized annually. Concurrently, four pairs of 10 m × 10 m ancillary plots were established nearby and one plot of each pair was also fertilized. In 2005, the fertilization experiment was extended to include all plots. Since then, one-half of each of the eight plots has received 112 kg ha^{-1} N annually in the form of NH_4NO_3.

Sampling regime. In each measurement campaign (Table 1), the aim was to sample needles from all four treatments and two canopy layers in as short time as possible. Except for the year 2008, the data from the unfertilized plots from the current dataset are also included in the synthesis paper by Ellsworth *et al.* (2012). The number of gas-exchange systems used (1–3) and of plot pairs sampled (1–5) varied by campaign. Sun- and shade-acclimated needles were sampled from the upper and lower thirds of the canopy, respectively. Depending on the season, current-year (autumn), 1-year-old needles (spring) or both age classes (summer)

TABLE 1. *Sampling regime, environmental conditions, and surface-area-based average nitrogen content*

Year	Sampling regime		n (n^*)				Sampling conditions		N_a	
	Date	Sampled plots	C	+N	+CO_2	+N+CO_2	T_L	D	C, +CO_2	+N, +N+CO_2
2002	6 October to 7 November	FACEp + ancillary ambient	13	15	6	6	19·8 (0·61)	1·08 (0·16)	1·19 (0·15)	1·59 (0·22)
2003	21 September to 3 November	FACEp + ancillary ambient	13	12	3	3	23·2 (2·12)	1·27 (0·27)	1·07 (0·22)	1·37 (0·25)
2004	1–18 June	FACEp	(5)	(7)	(8)	(7)	27·2 (2·32)	1·50 (0·27)	0·98 (0·15)	1·20 (0·20)
2008	2–9 September	FACE	8 (6)	6 (5)	6 (5)	6 (6)	27·8 (1·40)	1·36 (0·67)	0·88 (0·21)	0·94 (0·17)
									0·78 (0·13)	1·01 (0·22)

Sample size of current-year needles n (and 1-year-old needles n^*) specifies the number of curves per campaign and treatment combination included in the analysis. C stands for control plots, +N for fertilized plots, and +CO_2 is for plots with elevated atmospheric-CO_2 concentration. Also given are leaf temperature (T_L, °C,) and water vapour-pressure deficit (D, kPa) in the cuvette, and nitrogen content (N_a, g m^{-2}) of sun-acclimated needles averaged over all measurements (for N_a, by fertilization treatment) in each campaign (s.d. in parenthesis).

were sampled (Table 1). The central walk-up tower in each of the eight FACE plots, and a triangular tower in each ancillary plot, allowed access to the crowns of 1–5 trees in each treatment. Sampling order was randomized among treatments, plots within treatment, and trees within the plot. When possible, we sampled any individual tree only once in each campaign. When both age classes were measured, however, they were sampled from the same branch.

Gas-exchange measurements. All gas-exchange measurements were made with an open gas-exchange systems (Li-Cor 6400 with 6400-02B red/blue light source, and 20×30 mm chamber; Li-Cor Biosciences, Lincoln, NE, USA) on detached shoots (see Maier *et al.*, 2008; Drake *et al.*, 2010). From each sample, we measured a single '$A-c_i$ curve', i.e. the response of A to varying c_i, using the following procedure. The mid-sections of two or three fascicles were inserted in the leaf cuvette, where conditions were maintained at saturating light (1800 μmol m^{-2} s^{-1} PPFD), near ambient temperature, and within a narrow range in D (Table 1). After the gas-exchange rates were stabilized, at growth c_a, E and A were recorded at eight concentrations of c_a, between 60 and 1800 ppm.

After the gas-exchange measurements, needle length (mm) and diameter (mm) were measured to estimate total needle surface area, and the needle area in the chamber was used for rescaling the measured gas-exchange rates. The sampled fascicles were then oven-dried to constant mass at 65 °C (for 48 h), weighed and ground. Leaf mass per unit area (M_A, g m^{-2}) was calculated as the ratio of needle dry mass to total surface area. Needle N concentration was determined using a Carlo-Erba analyser (model NA 1500; Fison Instruments, Danvers, MA, USA).

Parameter estimation and other statistical analyses. The Farquhar-model parameters (Farquhar *et al.*, 1980; eqn 3), including $V_{c,max}$ were estimated from the $A-c_i$ curves following a fitting procedure similar to that described in Ellsworth *et al.* (2004). Our analysis focused on $V_{c,max}$, normalized to a standard temperature, $V_{c,max25}$, through the T_L-response function proposed by Campbell and Norman (1998). To minimize the possible bias in the values of the $A-c_i$ curve parameters caused by very low fluxes or a leaky chamber, an $A-c_i$ curve was omitted from the subsequent analysis if (*a*) the observed g_C changed >30 % during the measurements, (*b*) g_C was <0·03 mol m^{-2} s^{-1}, or (*c*) the intercept of the $A-c_i$ curve was more negative than −2·5 μmol m^{-2} s^{-1}.

The simplest approach to account for a saturating response of $V_{c,max25}$ to N_a is to assume a piecewise linear relationship, where N_p increases proportionally with N_a, $\partial N_p/\partial N_a = 1$, up to a transition point, after which it remains constant regardless of further increases in N_a. This piecewise representation implies that up to the transition point, the activation state of Rubisco either remains constant or its decrease is compensated by an increase in the fractional allocation to carboxylating enzymes. The transition point was not treated as a free parameter in the fitting, but rather set *a priori* at the N_a value where the value of the slope in the in the $V_{c,max25}-N_a$ relationship began to drop.

Estimates of WUE and PNUE were obtained from E and A measured at growth c_a. Marginal resource-use efficiencies were calculated using eqns (5), (8) and (11). For λ, the mean D for

the curve and c_i at growth c_a were used. For η, the curve-specific Farquhar-model parameters were used, with r set to 0·7 as determined from stable isotope measurements (Ellsworth *et al.*, 2012).

All following analyses rely on the assumption that CO_2 exchange is sensitive to fluctuations in stomatal conductance. However, note that the expressions for $V_{c,max}$ and its estimation method applied here are only valid when mesophyll conductance can be assumed to be non-limiting. Mesophyll conductance is partially explained by leaf structure, and studies on conifers (thick, dense leaves; Flexas *et al.*, 2008) suggest that the gas-phase limitations to A are small (<30 %) compared with internal limitations. Consequently, our estimated $V_{c,max}$ is better interpreted as a 'macroscopic' kinetic constant that also accounts for the internal diffusive limitations of leaves.

We looked for the treatment and age effects on functional relationships ($V_{c,max25}$ vs. N, and E vs. A) to identify the smallest number of distinct populations represented by the data. The largest number of possible populations is eight, i.e. two CO_2 concentrations, two N treatments and two age classes, and the smallest is one. Based on the extra-sum-of-squares principle (Ramsey and Schäfer, 1997), a single relationship presents a 'reduced' model, and a 'full' model includes different parameters for each sub-group. The difference in the mean squared error between full and reduced models was tested (F-test). All regressions were estimated using standard general linear models and least-square fitting procedures either in MatLab (MatLab 2009a; MathWorks, Natick, MA, USA) or Systat (Systat Software Inc., Richmond, CA, USA). Because our sampling regime was unbalanced, few statistical tests of the treatment effects on N_a and its dynamics can be performed.

RESULTS

Figure 1 shows how the range of foliar N concentrations and light-saturated photosynthetic rates measured (at growth c_a and various leaf temperatures) on leaves of single species and stand in this study relates to observations in a global dataset (Wright *et al.*, 2004). In the first two sampling years N_a of the fertilized current-year needles was 30 % higher compared with unfertilized needles in each CO_2 treatment (2002–2003; $n = 5$, maximum $P = 0{\cdot}01$, t-test). In 2008, based on a split-plot ANOVA (were c_a is the main effect and N availability the split-plot effect), fertilization increased the mean N_a of 1-year-old needles by 30 % ($n = 4$, maximum $P = 0{\cdot}03$). Finally, elevated c_a did not alter N_a of either age class (minimum $P = 0{\cdot}51$).

When scaled to a common leaf temperature (T_L) of 25 °C, the response of $V_{c,max}$ to N_a saturates for the current-year needles (Fig. 2A, B). For the linearly increasing part, where both age classes are presented, the intercept of the regression was lower for the current-year than the 1-year-old needles ($P < 0{\cdot}01$, ANCOVA). The driving variable was re-scaled to reflect the fraction of N that is photosynthetically active (N_p, Fig. 2C), such that when $N_a \leq 1{\cdot}4$ g m^{-2}, N_p increased linearly with N_a and, for $N_a > 1{\cdot}4$ g m^{-2}, N_p saturates with respect to N_a. Moreover, the $V_{c,max25}$–N_p relationship could be described with a single linear regression when N_p of 1-year-old needles was set to 0·9 of that in the current-year needles (Fig. 2D).

We found no fertilization effect on the $V_{c,max25}$–N_p response when evaluated for overlapping ranges in either growth c_a (minimum $P = 0{\cdot}58$, F-test for the difference between mean squared errors of reduced and full regression models). Also, elevated c_a did not affect the $V_{c,max25}$–N_p response in either age class (minimum $P = 0{\cdot}32$). Taken together, the slope of the $V_{c,max25}$–N_p relationship ($\partial a_1/\partial N_p$) could be described with a single temperature-dependent function (Fig. 2E). The residuals of the model showed no trends with N_a (Fig. 2F), T_L, and D (not shown).

We then assessed possible age and treatment effects on the relationship between E and A, and thus, WUE and λ_{LI}. In Fig. 3, to reduce the dimensions of the analysis, E is plotted as a function of $A_{380} \times D^{1/2}$, where A_{380} is CO_2 exchange rate measured at c_a of 380 μmol mol^{-1} across the treatments, and multiplication by $D^{1/2}$ allows interpreting the slope of the E-$A_{380} \times D^{1/2}$ relationship as the inverse of $\sqrt{(\lambda_{LI} c_a)}$ (eqn 6). Transpiration rate was approximately linearly related to

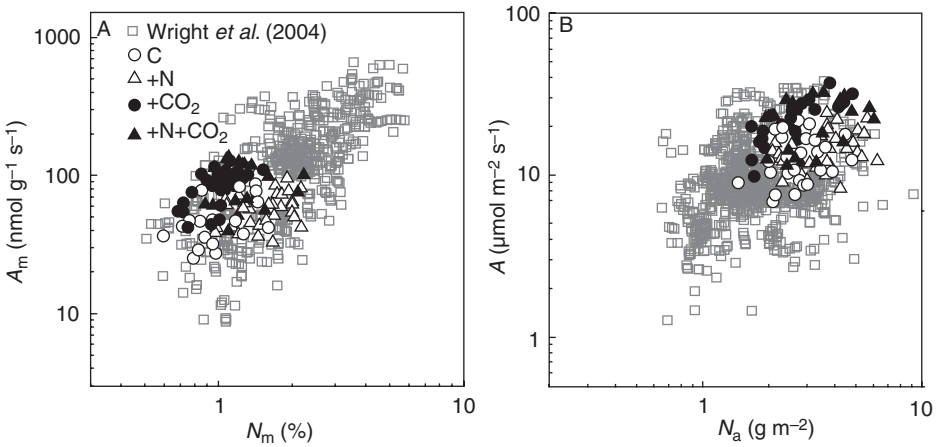

FIG. 1. (A) Relationship between light-saturated CO_2 exchange rate per unit leaf mass (A_m) and mass-based foliar nitrogen concentration (N_m), and (B) the same relationship when both variables are expressed on projected-area basis (A and N_a). Data from the global dataset of Wright *et al.* (2004) are indicated with grey boxes. Black symbols are data from this study of *Pinus taeda* from Duke FACE, where A_m and A are given at growth conditions, i.e. 380 and 580 μmol mol^{-1} for ambient (C, +N) and elevated atmospheric-CO_2 plots (+CO_2, +N + CO_2), respectively, and +N-elevated atmospheric CO_2 plots.

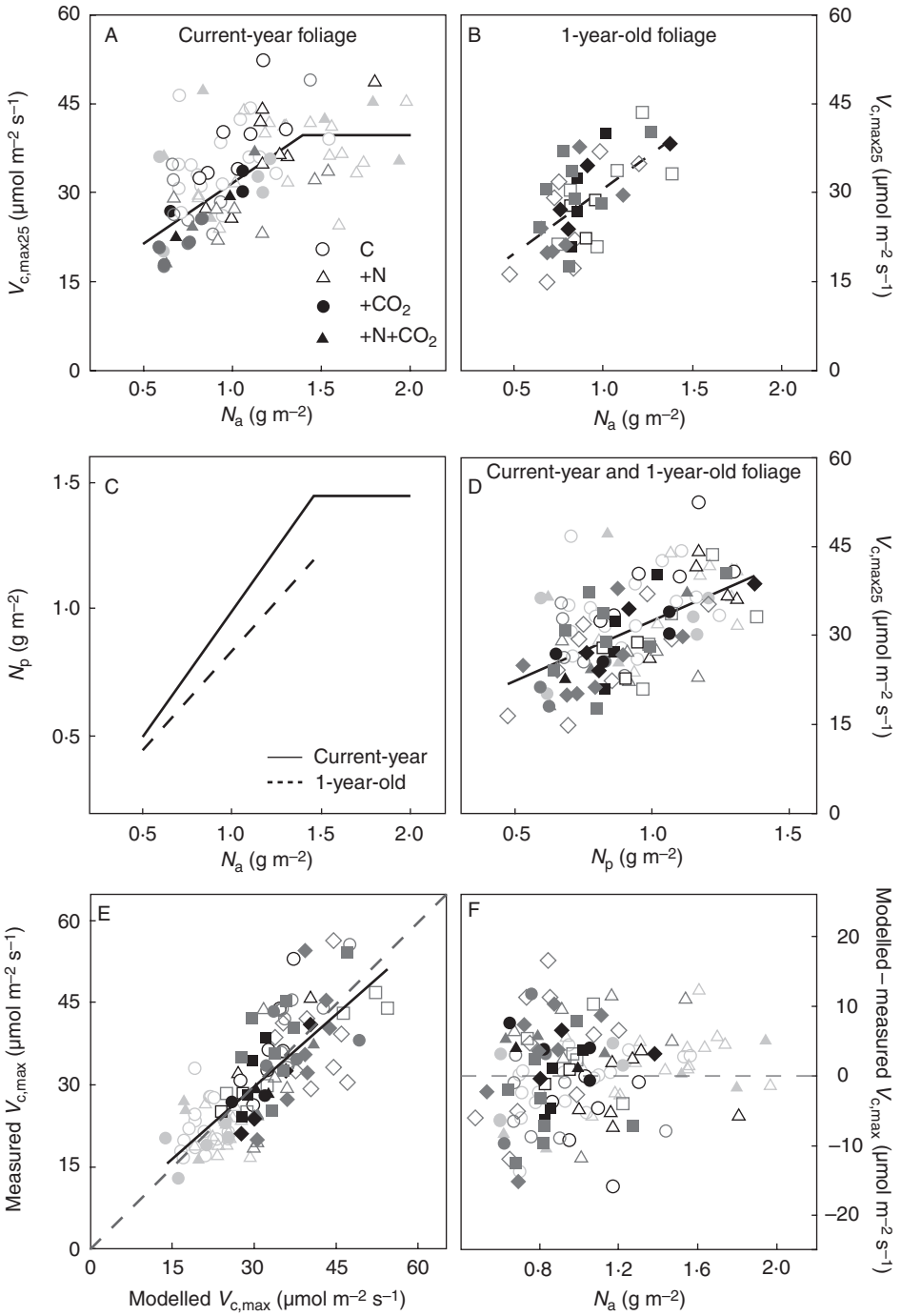

FIG. 2. (A) Maximum carboxylation rate scaled to a common leaf temperature (T_L) of 25 °C ($V_{c,max25}$) based on Campbell and Norman (1998) as a function of foliar nitrogen content (N_a) for current-year needles. (B) $V_{c,max25}$ as a function of N_a for 1-year-old needles. Squares indicate non-fertilized plots and diamonds are fertilized plots. Closed symbols stand for elevated atmospheric-CO_2 plots. (C) Photosynthetically active foliar nitrogen content (N_p) as a function of N_a. (D) $V_{c,max25}$ as a function of N_p (when $N_a \leq 1{\cdot}4$ g m^{-2}). (E) Measured vs. modelled $V_{c,max}$. Continuous and dashed lines represent regression ($R^2 = 0{\cdot}58$) and one-to-one lines, respectively. The intercept of the linear fit is not significantly different from zero ($P = 0{\cdot}29$). (F) Model residuals (modelled minus measured $V_{c,max}$) as a function needle nitrogen content (N_a). Symbols are as in Fig. 1, with shades of grey indicating different T_L ranges during measurements (light grey, $19 < T_L \leq 24$ °C; black, $24 < T_L \leq 26$ °C; dark grey, $26 \leq T_L \leq 30$ °C). Fitted functions ($P < 0{\cdot}01$): (A) $y = 11{\cdot}07 + 20{\cdot}60x$, $r^2 = 0{\cdot}48$, fit for data where $T_{leaf} > 24$ °C and $N_a \leq 1{\cdot}4$ g m^{-2}; (B) $y = 8{\cdot}79 + 22{\cdot}01x$, $r^2 = 0{\cdot}40$; (D) $y = 12{\cdot}76 + 20{\cdot}29x$, $r^2 = 0{\cdot}36$.

$A_{380} \times D^{1/2}$ across the sampled leaves, yet the slope appeared to vary with needle age and N content per unit leaf area. The water loss associated with a given CO_2 uptake was somewhat higher in 1-year-old compared with current-year needles ($P <$ 0·01, F-test). Nitrogen fertilization did not change the E–$A_{380}D^{1/2}$ relationship in either needle age class or growth c_a (minimum $P = 0{\cdot}31$, F-test). Nevertheless, when the data for current-year needles were grouped by N_a (high and low;

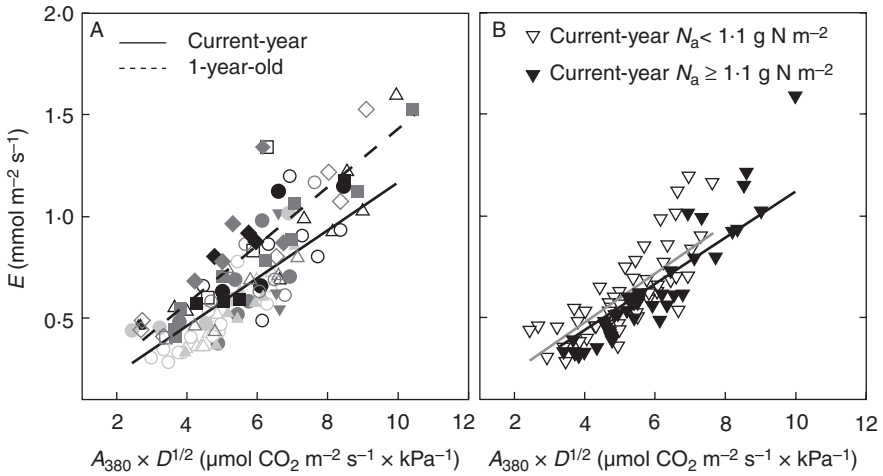

FIG. 3. (A) Transpiration rate (E) as a function of $A_{380} \times D^{1/2}$, where CO_2 exchange rate (A) is taken at a common c_a of 380 μmol mol^{-1} CO_2. Symbols as in Fig. 2. (B) E as a function of $A_{380} \times D^{1/2}$ for current-year needles; the data are binned by leaf nitrogen content (N_a). Fitted lines: (A) $y = 0{\cdot}12x$ (continuous); $y = 0{\cdot}14x$ (dashed); (B) $y = 0{\cdot}11x$ (black); $y = 0{\cdot}12x$ (grey).

Fig. 3B), needles in the high-N_a group (including sun-acclimated needles across treatments) fixed slightly more CO_2 at any given E loss ($P = 0{\cdot}01$, F-test).

PNUE and WUE were inversely correlated ($P < 0{\cdot}01$; Fig. 4). To provide a context for this negative correlation, we note that, by definition, PNUE = WUE (E/N). Hence, for a constant E/N, any correlation between PNUE and WUE must be positive. It follows that the inverse correlation between PNUE and WUE must originate from an inverse correlation between variations in E versus N implying N and water trade-off. This trade-off is better revealed when marginal N and water-use efficiencies are used (Fig. 5A; eqn 11), as these quantities are not affected by the measurement conditions. Note that in Figs 4 and 5, WUE and λ_{LI} were scaled by c_a to account for the effect of c_a on A. Complementarity is expected between η_{LI} and the square root of λ_{LI} since both sides of eqn (11) depend on c_i in opposite ways. A similar dependence of η on λ_{LI} is obtained when the optimality assumption is relaxed and the full version of eqn (8) is used in estimating η (Fig. 5B). The term denoted as T_2 in eqn (8) accounts for possible variations in c_i originating from N_p at a given stomatal conductance and was always negative. The ratio T_2/T_1 decreased with increasing N_p and averaged at −0·33 and −0·22 for needles grown under ambient and elevated c_a, respectively, explaining the downward shift and larger variability in estimates of η (as compared with η_{LI}) at each λ_{LI} (Supplementary Data online).

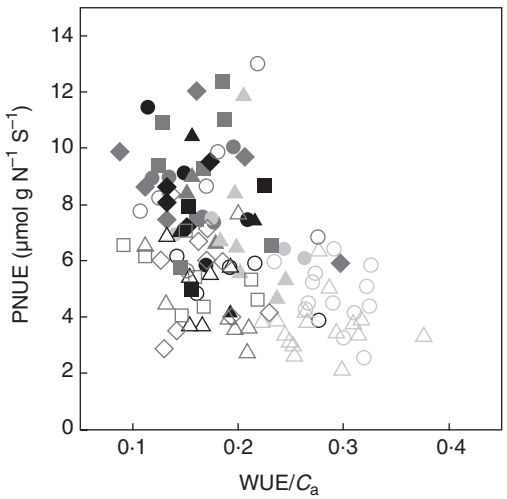

FIG. 4. Nitrogen-use efficiency [PNUE, the ratio of light-saturated CO_2 exchange rate (A) to needle nitrogen content = A/N] as a function of water-use efficiency (WUE, the ratio of A to transpiration rate = A/E) scaled by the atmospheric-CO_2 concentration (380 and 580 μmol mol^{-1} for the ambient and elevated treatments, respectively). Each point represents one needle sample. Symbols are as in Fig. 2.

DISCUSSION

In this study, we presented a simplified analytical scaling rule that relates marginal N and water-use efficiencies (respectively η_{LI} and λ_{LI}), the values of which can be readily derived from measured $A-c_i$ curves and foliar N. The wide range of A and N found among trees grown at Duke FACE allowed the link between η_{LI} and λ_{LI} and the effects of elevated CO_2 and site N fertility on the relationship to be characterized.

The mass-based foliar N concentration (N_m), the leaf-mass-to-area ratio (M_A) and their product, N_a, vary considerably across biomes, functional types and within a stand (Wright *et al.*, 2004; Fig. 1). The large variability in N_m and especially N_a in our dataset has two sources: the availability of light and N. The physiological implications of variability in these two resources, as reflected in the within-canopy distribution of nitrogen and carbon and among various pools, can be quite different (Niinemets and Tenhunen, 1997). First, we sampled needles from various heights in the canopy to capture the range in N_a induced by variation in light environment: while N_m varied little among canopy positions, N_a decreased as M_A decreased with decreasing light availability (data not shown). Secondly, the Duke FACE stand is

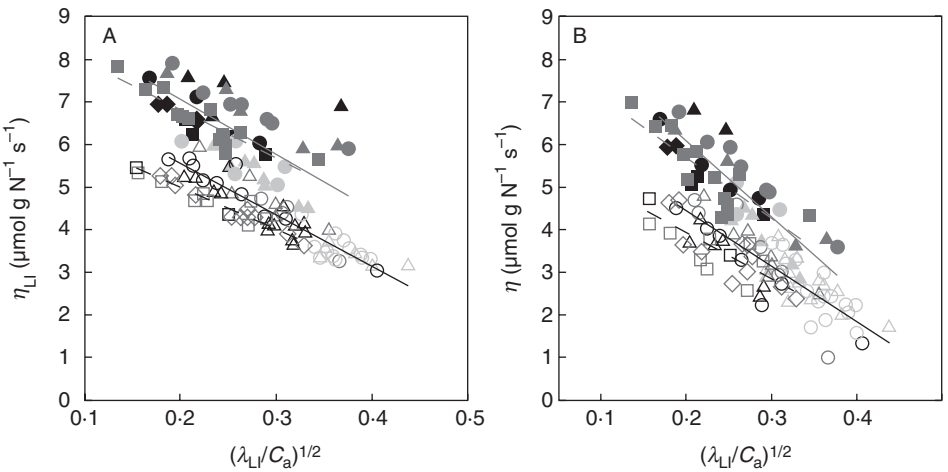

FIG. 5. Relationship between marginal nitrogen-use efficiency (η) and marginal water-use efficiency (λ), (A) assuming an optimal stomatal conductance (i.e. computing η_{LI} via eqn 11), and (B) in the most general case (i.e. employing eqn 8 to compute η). λ_{LI} is scaled by the atmospheric CO_2 concentration (c_a; 380 and 580 μmol mol^{-1} for the ambient and elevated treatments, respectively). Each point represents one needle sample. Symbols are as in Fig. 2. Black and grey lines are linear fits for data from ambient and elevated atmospheric-CO_2 plots, respectively, and continuous and broken lines for current and 1-year-old needles, respectively.

growing on relatively poor soil and N fertilization increased N_a, particularly in the early years of N amendments (Table 1). Thus, approx. 95 % of the temporal variation in the mean N_a is explained by variation in N_m.

Driven by data from sun-acclimated needles of fertilized trees collected in the earlier years of the study (2002–2003), the response of $V_{c,max}$ to N_a when scaled to a common T_L of 25 °C saturates for the current-year needles (Fig. 2A). Discounting the photosynthetically inactive N when exceeding 1·4 g m^{-2} (Fig. 2C) and lower N_p of 1-year-old needles, the $V_{c,max25}$–N_p relationship could be described with a single linear regression (Fig. 2D). Fertilization did not significantly affect the $V_{c,max25}$–N_p relationship in either growth c_a. The growth c_a, in turn, did not affect the relationship in either age class. Thus, the slope of the $V_{c,max25}$–N_p relationship had a single temperature-dependent function (Fig. 2E). Therefore, accounting for the photosynthetically active N, and the varying leaf temperature, explains much of the variation of A versus N_a (Fig. 1) and facilitates the estimation of η_{LI}.

Our data expands the large dataset of gas-exchange data collected at Duke FACE (Crous *et al.*, 2008; Maier *et al.*, 2008; Ellsworth *et al.*, 2012), and adds to the small amount of data available from the elevated $c_a \times$ N experiments. Regardless of treatment, the rate of change in $V_{c,max}$ with N_a observed in the current study agrees with the earlier data from the unfertilized Duke FACE plots (Ellsworth *et al.*, 2012), but extends the range to $N_a > 1{\cdot}5$ g m^{-2}, thus, beyond previously observed values. Also, consistent with previous findings on *P. taeda* at this site, no acclimation of photosynthesis to elevated c_a was found in current-year needles. For 1-year-old needles, however, Crous *et al.* (2008) showed a downward shift in the $V_{c,max}$–N_a response for needles grown under elevated c_a, compared with needles grown under ambient c_a, but no shift when the trees received additional N. The down-regulation of Rubisco in response to c_a can be accounted for in the present framework as a reduction in $\partial a_1/\partial N_a$ and η_{LI}.

As observed in other studies (DeLucia and Schlesinger, 1991; Cernusak *et al.*, 2008; Han, 2011) PNUE and WUE were inversely related (Fig. 4). The rather large variability in the flux-based efficiency estimates is due to variation in T_L and D thus weakening the expected inverse correlation between them (Wright *et al.*, 2003). However, both PNUE and WUE consistently increased with elevated c_a, due to larger A for given E and leaf N. Han (2011) studied changes in water and N use with height in the tree (at constant light availability), and found that both N_m and N_a increased, but stomatal conductance decreased with height, and that light-saturated A was inversely correlated with N_a. This implies that the limited water available to taller trees (hydraulic limitation) increased the N cost associated with carbon gain and lead to a trade-off between PNUE and WUE. In our dataset, an analysis of the E–$A_{380} \times D^{1/2}$ response (similar to one in Fig. 3) revealed that WUE and λ_{LI} were similar for the upper and lower thirds of the canopy. However, height and light availability co-vary in our study and their effects on stomatal conductance are therefore inseparable.

As predicted by eqn (11), η_{LI} and λ_{LI} were inversely related (Fig. 5A). The values of λ_{LI} and η_{LI} were computed using eqns (5) and (11), therefore assuming that $\partial c_i/\partial N_p = 0$ (i.e. at optimal stomatal conductance). Both η_{LI} and λ_{LI} vary with c_i and, when plotted against each other, the data split into various groups based on growth c_a, N_a and needle age. Up to relatively high nitrogen content per unit leaf area ($N_a \leq 1{\cdot}4$ g m^{-2}), η_{LI} and $\lambda_{LI}^{1/2}$ are complementary, and elevated c_a shifts the relationship upwards. At the higher end of the observed N_a, $\eta_{LI} = 0$ (points not shown in Fig. 5), because of the chosen piecewise linear model that relates changes in N_p to those in N_a. This approximation may mask a more realistic scenario where, at a given c_a, each additional increase in N_a results in diminishing returns in terms of CO_2 uptake. Lastly, due to age-related decline in photosynthetically active N, η_{LI} was somewhat, but not consistently, lower in 1-year-old than in current-year needles.

We computed η_{LI} first by assuming the needles were operating at their optimal stomatal conductance, i.e. that c_i changes predictably with D but not with N_p. To assess the consequences of this assumption, to estimate η, we used the full version of eqn (8), where T_2 accounts for possible variations in c_i originating from N_a at a given stomatal conductance (see Fig. 3). T_2 becomes important for computing η, if a change in N_a causes a relative change in c_i comparable to the relative change in carboxylation rate ($V_{c,max}$). The results indicate that this may indeed be the case under certain conditions, in particular at high N_a. It also implies that the marginal water-use efficiency tends to increase with N_a, reflecting a larger $c_a - c_i$ gradient and CO_2 uptake at a given transpiration rate (Fig. 3B; Supplementary Data). This suggests that stomata may not be operating strictly optimally in terms of carbon-gain and water-loss economy, as predicted by the current objective function. This optimality model does not explicitly include N limitation and may also need to be constrained by leaf structural properties, such as plasticity in leaf mass per area.

Conclusions

On the basis of the optimal stomatal control theory and a linearized CO_2-demand function at the photosynthetic site, we obtained an analytical relationship between marginal water and N-use efficiency that implies complementarity between these two quantities. Data collected in a *P. taeda* canopy supported the model predictions, exhibiting scaling between marginal N- and water-use efficiencies, thus allowing derivation of one quantity from the other. Future work should assess situations where linearized CO_2 demand function cannot be assumed. For *P. taeda* these include lower than saturating light availability and higher atmospheric [CO_2] than that targeted in the Duke FACE experiment. In search of a better description of the optimization problem plants are facing, the proposed approach can be used to evaluate the generality of the current findings. Comparisons across species and growth environments would be useful for this, particularly where marginal water-use efficiency reflects the growth environment through leaf hydraulic and structural properties, e.g. foliar N and mass-to-area ratio, and marginal N-use efficiency through allocation of foliar N to photosynthetic machinery.

SUPPLEMENTARY DATA

Supplementary data are available online at www.aob.oxfordjournals.org and consists of an assessment of the relative importance of Terms 1 and 2 (T_1 and T_2 in eqn 8) when estimating marginal N-use efficiency.

ACKNOWLEDGEMENTS

This work was partially supported by the US Department of Agriculture (grant numbers 2011-67003-30222 and FS-AGRMNT 09-CA-11330140-059), the US Department of Energy (DOE) through the Office of Biological and Environmental Research (BER) Terrestrial Carbon Processes (TCP) program (grant numbers DE-FG02-95ER62083 and DE-FC02-06ER64156), the National Science Foundation (grant numbers NSF-EAR-10-13339, NSF-AGS-11-02227 and NSF-CBET-10-33467) and the Binational Agricultural Research Development fund (grant number IS-4374-11C).

LITERATURE CITED

Ainsworth EA, Rogers A. 2007. The response of photosynthesis and stomatal conductance to rising [CO_2]: mechanisms and environmental interactions. *Plant, Cell & Environment* **30**: 258–270.

Anten NPR, Schieving F, Werger MJA. 1995. Patterns of light and nitrogen distribution in relation to whole canopy carbon gain in C-3 and C-4 monocotyledonous and dicotyledonous species. *Oecologia* **101**: 504–513.

Barton CVM, Duursma RA, Medlyn BE, *et al*. 2012. Effects of elevated atmospheric [CO2] on instantaneous transpiration efficiency at leaf and canopy scales in *Eucalyptus saligna*. *Global Change Biology* **18**: 585–595.

Bloom AJ, Sukrapanna SS, Warner RL. 1992. Root respiration associated with ammonium and nitrate absorption and assimilation by barley. *Plant Physiology* **99**: 1294–1301.

Bonan GB. 2008. Forests and climate change: forcings, feedbacks, and the climate benefits of forests. *Science* **320**: 1444–1449.

Buckley TN. 2008. The role of stomatal acclimation in modelling tree adaptation to high CO_2. *Journal of Experimental Botany* **59**: 1951–1961.

Buckley TN, Miller JM, Farquhar GD. 2002. The mathematics of linked optimisation for water and nitrogen use in a canopy. *Silva Fennica* **36**: 639–669.

Campbell GS, Norman JM. 1998. *An introduction to environmental biophysics*, 2nd edn. New York, NY: Springer-Verlag.

Cernusak LA, Winter K, Aranda J, Turner BL. 2008. Conifers, angiosperm trees, and lianas: growth, whole-plant water and nitrogen use efficiency, and stable isotope composition (delta C-13 and delta O-18) of seedlings grown in a tropical environment. *Plant Physiology* **148**: 642–659.

Cheng LL, Fuchigami LH. 2000. Rubisco activation state decreases with increasing nitrogen content in apple leaves. *Journal of Experimental Botany* **51**: 1687–1694.

Cowan I, Farquhar GD. 1977. Stomatal function in relation to leaf metabolism and environment. *Symposia of the Society for Experimental Biology* **31**: 471–505.

Crous KY, Ellsworth DS. 2004. Canopy position affects photosynthetic adjustments to long-term elevated CO_2 concentration (FACE) in aging needles in a mature *Pinus taeda* forest. *Tree Physiology* **24**: 961–970.

Crous KY, Walters MB, Ellsworth DS. 2008. Elevated CO_2 concentration affects leaf photosynthesis–nitrogen relationships in *Pinus taeda* over nine years in FACE. *Tree Physiology* **28**: 607–614.

DeLucia EH, Schlesinger WH. 1991. Resource-use efficiency and drought tolerance in adjacent Great-Basin and Sierran plants. *Ecology* **72**: 51–58.

Dewar RC, Franklin O, Makela A, McMurtrie RE, Valentine HT. 2009. Optimal function explains forest responses to global change. *Bioscience* **59**: 127–139.

Dewar RC, Tarvainen L, Parker K, Wallin G, McMurtrie RE. 2012. Why does leaf nitrogen decline within tree canopies less rapidly than light? An explanation from optimization subject to a lower bound on leaf mass per area. *Tree Physiology* **32**: 520–534.

Drake JE, Raetz LM, Davis SC, DeLucia EH. 2010. Hydraulic limitation not declining nitrogen availability causes the age-related photosynthetic decline in loblolly pine (*Pinus taeda* L.) *Plant, Cell & Environment* **33**: 1756–1766.

Ellsworth DS, Reich PB, Naumburg ES, Koch GW, Kubiske ME, Smith SD. 2004. Photosynthesis, carboxylation and leaf nitrogen responses of 16 species to elevated pCO_2 across four free-air CO_2 enrichment experiments in forest, grassland and desert. *Global Change Biology* **10**: 2121–2138.

Ellsworth DS, Thomas R, Crous KY, *et al*. 2012. Elevated CO_2 effects on photosynthetic responses to light and [CO_2] over ten years: a synthesis from Duke FACE. *Global Change Biology* **18**: 223–242.

Ethier GJ, Livingston NJ, Harrison DL, Black TA, Moran JA. 2006. Low stomatal and internal conductance to CO_2 versus Rubisco deactivation as determinants of the photosynthetic decline of ageing evergreen leaves. *Plant, Cell & Environment* **29**: 2168–2184.

Evans JR. 1989. Photosynthesis and nitrogen relationships in leaves of C-3 plants. *Oecologia* **78**: 9–19.

Farquhar GD, von Caemmerer S, Berry JA. 1980. A biochemical model of photosynthetic CO_2 assimilation in leaves of C3 species. *Planta* **149**: 78–90.

Farquhar GD, Buckley TN, Miller JM. 2002. Optimal stomatal control in relation to leaf area and nitrogen content. *Silva Fennica* **36**: 625–637.

Field C. 1983. Allocating leaf nitrogen for the maximization of carbon gain: leaf age as a control on the allocation program. *Oecologia* **56**: 341–347.

Field C, Mooney HA. 1986. The photosynthesis–nitrogen relationship in wild plants. In: Givnish TJ. ed. *On the economy of plant form and function*. Cambridge: Cambridge University Press, 25–55.

Field C, Merino J, Mooney HA. 1983. Compromises between water-use efficiency and nitrogen-use efficiency in 5 species of California evergreens. *Oecologia* **60**: 384–389.

Flexas J, Ribas-Carbo M, Diaz-Espejo A, Galmes J, Medrano H. 2008. Mesophyll conductance to CO_2: current knowledge and future prospects. *Plant, Cell & Environment* **31**: 602–621.

Han Q. 2011. Height-related decreases in mesophyll conductance, leaf photosynthesis and compensating adjustments associated with leaf nitrogen concentrations in *Pinus densiflora*. *Tree Physiology* **31**: 976–984.

Hari P, Mäkelä A, Korpilahti E, Holmberg M. 1986. Optimal control of gas exchange. *Tree Physiology* **2**. 169–176.

Katul GG, Palmroth S, Oren R. 2009. Leaf stomatal responses to vapour pressure deficit under current and CO_2-enriched atmosphere explained by the economics of gas exchange. *Plant, Cell & Environment* **32**: 968–979.

Katul GG, Manzoni S, Palmroth S, Oren R. 2010. A stomatal optimization theory to describe the effects of atmospheric CO_2 on leaf photosynthesis and transpiration. *Annals of Botany* **105**: 431–442.

Kull O, Kruijt B. 1999. Acclimation of photosynthesis to light: a mechanistic approach. *Functional Ecology* **13**: 24–36.

Launiainen S, Katul GG, Kolari P, Vesala T, Hari P. 2011. Empirical and optimal stomatal controls on leaf and ecosystem level CO_2 and H_2O exchange rates. *Agricultural and Forest Meteorology* **151**: 1672–1689.

Lloyd J. 1991. Modeling stomatal responses to environment in *Macadamia integrifolia*. *Australian Journal of Plant Physiology* **18**: 649–660.

McMurtrie RE, Norby RJ, Medlyn BE, *et al*. 2008. Why is plant-growth response to elevated CO_2 amplified when water is limiting, but reduced when nitrogen is limiting? A growth-optimisation hypothesis. *Functional Plant Biology* **35**: 521–534.

McMurtrie R, Wolf L. 1983. Above-ground and below-ground growth of forest stands: a carbon budget model. *Annals of Botany* **52**: 437–448.

Maier CA, Palmroth S, Ward E. 2008. Short-term effects of fertilization on photosynthesis and leaf morphology of field-grown loblolly pine following long-term exposure to elevated CO_2 concentration. *Tree Physiology* **28**: 557–606.

Manzoni S, Katul G, Fay PA, Polley HW, Porporato A. 2011*a*. Modeling the vegetation-atmosphere carbon dioxide and water vapor interactions along a controlled CO_2 gradient. *Ecological Modelling* **222**: 653–665.

Manzoni S, Vico G, Katul GG, *et al*. 2011*b*. Optimizing stomatal conductance for maximum carbon gain under water stress: a meta-analysis across plant functional types and climates, *Functional Ecology*, **25**: 456–467.

Medlyn BE, Barton CVM, Broadmeadow MSJ, *et al*. 2001. Stomatal conductance of forest species after long-term exposure to elevated CO_2 concentration: a synthesis. *New Phytologist* **149**: 247–264.

Medlyn BE, Duursma RA, Eamus D, *et al*. 2011. Reconciling the optimal and empirical approaches to modelling stomatal conductance. *Global Change Biology* **17**: 2134–2144.

Niinemets U, Tenhunen JD. 1997. A model separating leaf structural and physiological effects on carbon gain along light gradients for the shade-tolerant species *Acer saccharum*. *Plant, Cell & Environment* **20**: 845–866.

Ollinger SV, Richardson AD, Martin ME, *et al*. 2008. Canopy nitrogen, carbon assimilation, and albedo in temperate and boreal forests: functional relations and potential climate feedbacks. *Proceedings of the National Academy of Sciciences of the USA* **105**: 19336–19341.

Palmroth S, Berninger F, Nikinmaa E, Lloyd J, Pulkkinen P, Hari. 1999. Structural adaptation rather than water conservation was observed in Scots pine over a range of wet to dry climates. *Oecologia* **121**: 302–309.

Peltoniemi MS, Duursma RA, Medlyn BE. 2012. Co-optimal distribution of leaf nitrogen and hydraulic conductance in plant canopies. *Tree Physiology*, **32**: 510–519.

Ramsey F, Schafer D. 1997. *The statistical sleuth: a course in methods of data analysis.* San Francisco, CA: Duxbury Press.

Rogers A, Ellsworth DS. 2002. Photosynthetic acclimation of *Pinus taeda* (loblolly pine) to long-term growth in elevated pCO_2 (FACE). *Plant, Cell & Environment* **25**: 851–858.

Volpe V, Manzoni S, Marani M, Katul GG. 2011. Leaf conductance and carbon gain under salt-stressed conditions, *Journal of Geophysical Researach* **116**: G04035. http://dx.doi.org/10.1029/2011JG001848.

Warren CR, Dreyer E, Adams MA. 2003. Photosynthesis–Rubisco relationships in foliage of *Pinus sylvestris* in response to nitrogen supply and the proposed role of Rubisco and amino acids as nitrogen stores. *Trees – Structure and Function* **17**: 359–366.

Way DA, Oren R, Kim HS, Katul GG. 2011. How well do stomatal conductance models perform on closing plant carbon budgets? A test using seedlings grown under current and elevated air temperatures. *Journal of Geophysical Research-Biogeosciences* **116**: pG04031. http://dx.doi.org/10.1029/2011JG001808.

Wright IJ, Reich PB, Westoby M. 2003. Least-cost input mixtures of water and nitrogen for photosynthesis. *American Naturalist* **161**: 98–111.

Wright IJ, Reich PB, Westoby M, *et al* 2004. The worldwide leaf economics spectrum. *Nature* **428**: 821–827.